Physics and Performance Optimization of Electronic Paper

Richard C. Lean
Briarcliff Manor, New York

The physics of two versions of reflective electronic papers: E-Ink™ and Gyricon™ are examined. Electrodynamic models are developed to understand their design and to optimize performance. Models are verified with analytic solutions, published data, and laboratory experiments to ensure fidelity and accuracy. Excellent agreement is obtained using a set of self-consistent parameters. Specific engineering suggestions are proposed to: lower switching voltage, reduce switching time, improve display resolution, control Gyricon charging, and create gray level images.

Journal of Imaging Science and Technology 46: 562–574 (2002)

Introduction

Electronic paper refers to an innovative display medium that is thin, lightweight, electrically refreshable, robust, inexpensive, and operates with low power. Early uses range from advertising signs at 2 dpi (dots/inch) resolution to monochrome PDA and E-book displays at 70–80 dpi (Figures 1 and 2). Future trends point to color laptop and wireless wide area displays. Electronic paper technologies are broadly classified as emissive or reflective. Emissive technologies convert electrical power into light energy with an efficiency of 5%. Uniax Corporation uses electroluminescent light-emitting polymer[1] (LEP) with semiconductive properties. When a voltage is applied, the material emits visible light of intensities that comparable to those of inorganic light-emitting diodes (LED). Liquid crystal displays (LCD) from Minolta work on the principle of using an electric (**E**) field to rotate a liquid crystal molecule, leading to the polarization of light. Backlighting is required as the coefficient of transmission is less than 0.2. Sharp eliminates backlighting by using cholesteric liquid crystals and polymer materials (monoacrylate) with bistable properties for a reflection type display[2] that has two electrically switchable states: a planar transparent and a conic scattering state. Bell Labs uses a light sensitive protein called bacteriorhodopsin (BR), made by a saltwater bacterium (*Halobacterium salinarium*), which efficiently converts light energy into electric energy.[3] The electric fields, **E**, induce deprotonization resulting in a shift of the optical absorption peak[4] enabling this technology to be used as a reflective electronic display.[5] Two recent promising commercial efforts are E-Ink™ from E-Ink Corporation[6,7] and Gyricon™ from Gyricon Media Inc.[8,9]

Original manuscript received November 12, 2001

*Corresponding author rlean@mit.edu

E-Ink Display

E-Ink consists of white pigment balls in a dielectric blue dye that displaces to an **E** field (Fig. 1). In this electrophoretic device, the **E** field causes charge separation and displacement of both the positively charged white pigment and the much smaller negatively charged transparent micelles, or counterions. Each electrode controls an area coated with a monolayer of capsules about 120 μm in diameter for an image resolution of 220 dpi. The fabrication process includes spreading a monolayer of these capsules onto a substrate, drying, adhesion, and compression between transparent electrodes, resulting in a pancake with an approximately hexagonal closed-packed distribution. The electrodes may be formed from NESA (conductive coated) glass or Indium Tin Oxide (ITO) coated plastics. The capsule is electrically neutral before a bias **E** field is applied, and charge is conserved after application of the field. Other variations of E-Ink include opposite charged white and colored pigments in an inert colorless fluid.

Gyricon Display

Gyricon consists of bichromal balls in oil-filled spherical cavities that rotate when an **E** field is applied (Fig. 2). The oil acts to coat, insulate, and lubricate the ball, which is white on one side and colored on the other. The two hemispheres are chemically charged differently to create an electric dipole. When an **E** field is applied, the induced torque rotates the ball to align with the field, making the Gyricon a nonvolatile display. At a ball diameter of 40 μm, a resolution of 660 dpi is possible. Balls are fabricated using a 2 to 3 inch diameter disk spinning at 2000 to 20,000 rpm.[10] Pigmented carnauba wax from the leaves of the Brazilian palm tree (*Copenica Cerifera*), is fed from both sides towards the center of the spinning disc where they creep to the rim and form finger-like projections. Through a balance of viscous stress, surface tension, and centrifugal force, capillary instability leads to break up of these projections

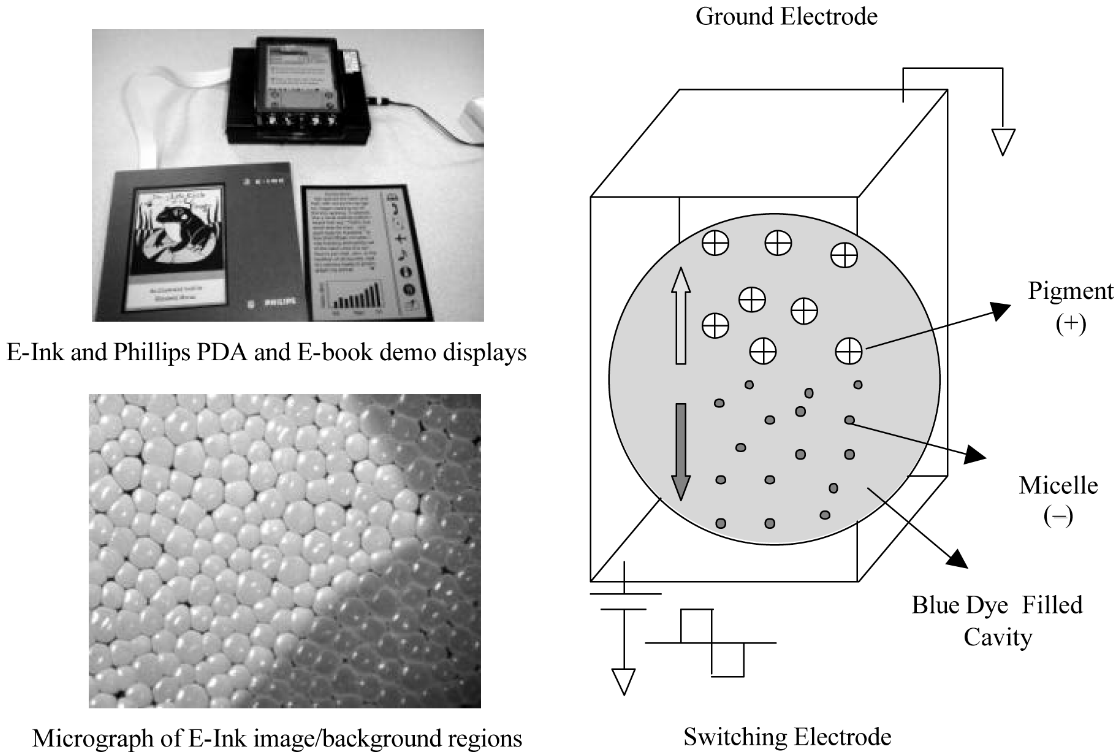

Figure 1. E-Ink applications, micrograph, and perspective view of 3D display cell operation

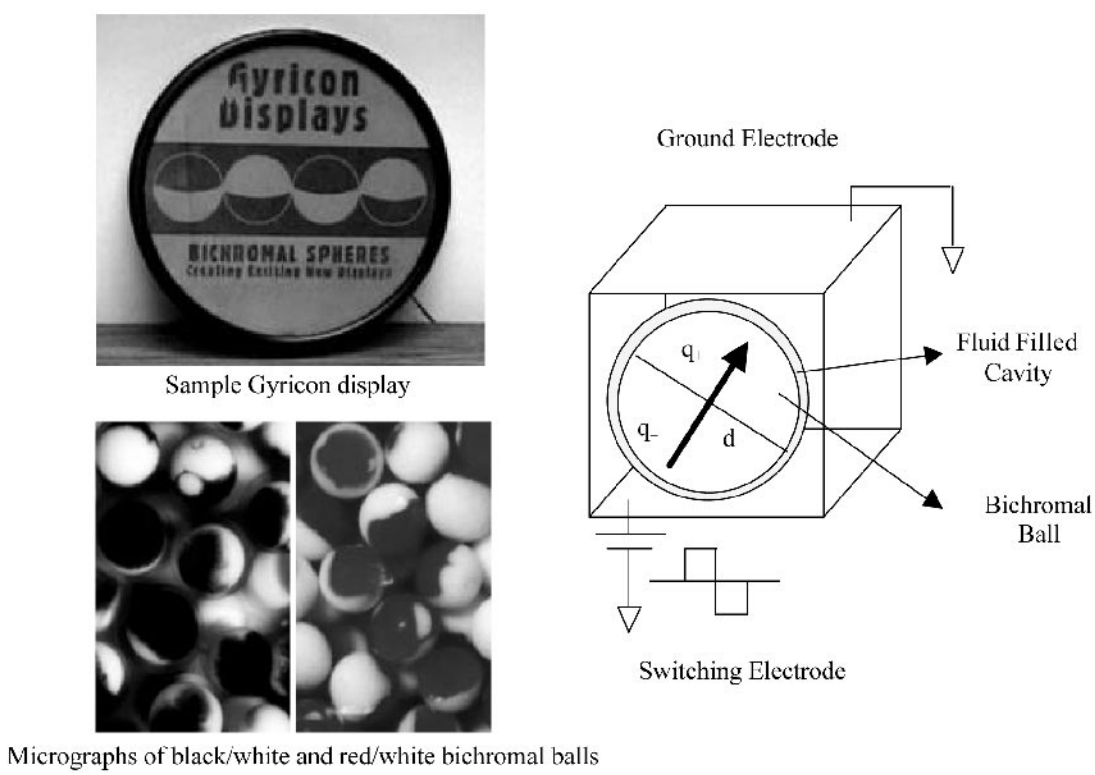

Figure 2. Gyricon application, micrographs, and perspective view of 3D display cell operation

to create perfectly spherical drops formed from two hemispheres, which cool rapidly and solidify during flight. Titanium dioxide is used as a pigment for the white color. The balls are then dispersed in viscous silicone oil, formed into transparent sheets, and heat cured to result in a thin but tough elastomer film. The opposing charge on the hemispheres is approximately equal for pure rotation, but translation may occur when the charge is unbalanced.

This work examines the physics and develops three-dimensional numerical models to simulate the electrodynamic performance of both E-Ink and Gyricon displays. Models are verified against analytic solutions, published results, and laboratory experiments to ensure fidelity and accuracy. Solution dynamics are animated using a graphics package from Advanced Visual Systems[11] (AVS) to compare against video from laboratory experiments. The verified models are then used as engineering design tools to optimize the performance of both display devices.

Problem Formulation and Model Descriptions

The physics of E-Ink and Gyricon display operation depends on electrostatic forces and torques to create translational and/or rotational motion. The two governing equations are Poisson's equation for electrostatic fields[12] and Newton's equation of motion. Poisson's equation, $\nabla \bullet \mathbf{E} = \rho/\varepsilon_o$, guarantees charge conservation where ρ is the charge density, and ε_o the permittivity of free space. The bichromal Gyricon ball has a dipole moment, $\mathbf{p}$, given by $\mathbf{p} = q\mathbf{d}$ with d being the ball diameter, and q the hemisphere charge. Dipole rotation is tracked by following the two spherical coordinate angles: θ and ψ. The polarization energy, $U = -\mathbf{p} \bullet \mathbf{E}$, is a minimum at equilibrium so that it provides a convenient check for time-dependent convergence of the dipole orientation.

Translational Motion

E-Ink pigment motion and Gyricon ball translation are governed by Newton's equation:

$$m\, d\mathbf{v}/dt = q\mathbf{E} + (\mathbf{p} \bullet \nabla)\mathbf{E} - 6\pi\eta r\mathbf{v} \qquad (1)$$

where m, r, $\mathbf{v}$, and η, is respectively mass, radius, velocity, and viscosity. The first term on the right is the Coulomb force due to the presence of an electrostatic field. The second term is a dipole force, which vanishes in a uniform field. The third term is Stoke's drag for a sphere.

Rotational Motion

Gyricon ball rotation is governed by the torque equation:

$$\mathbf{r}\ x\ m d\omega/dt = \mathbf{p} \text{ x } \mathbf{E} - k\ 4\pi\eta r^2\omega \qquad (2)$$

where $\mathbf{r}$ and ω are respectively, radial vector from the ball centroid and angular velocity. The first term on the right is the torque on the ball. The second term represents viscous damping, or friction. The viscous damping constant, k, depends on material and operational properties. Sheridon[8] referenced a more complicated expression for the viscous drag term:

$$D_v = r_b^3 r_c/(r_b - r_c)\ \eta\omega \ln[2r_b(r_c - r_b)/r_c t] + k\ r_b^3\eta\omega \qquad (3)$$

where r_b and r_c are the radius of the ball and cavity, and t is the smallest separation between the ball and cavity surfaces. The first term is ignored in this first-order approximation.

Time Integration Algorithm

Forward and backward difference formulae are used for time integration of the second order equation for a vector, $\mathbf{r}$, to derive:

$$d^2\mathbf{r}/dt^2 = [\mathbf{r}(t+\Delta t) - 2\ \mathbf{r}(t) + \mathbf{r}(t - \Delta t)]\ /\Delta t^2 \qquad (4)$$

Iterative forms of Eqs. (1) and (2) with force, $\mathbf{F}$, and torque, $\mathbf{T}$, are:

$$\mathbf{r}(t+\Delta t) = 2\ \mathbf{r}(t) - \mathbf{r}(t - \Delta t) + [\mathbf{F}(t) - 6\pi\eta r\ d\mathbf{r}/dt]/m\Delta t^2$$
$$\lambda(t+\Delta t) = 2\ \lambda(t) - \lambda(t - \Delta t) + [\mathbf{T}(t) - k\ 4\pi\eta r^3\ d\lambda/dt]/mr^2\ \Delta t^2 \qquad (5)$$

Given $\mathbf{r}(t)$, $\mathbf{r}(t - \Delta t)$, and $\mathbf{F}(t)$, the linear displacement $\mathbf{r}(t + \Delta t)$ can be calculated at the next time level. Similarly considerations apply for angular displacement $\lambda(t + \Delta t)$.

Validation of Numerical Models

Solutions are generated with both models for verification.

Sample Calculation with 3-Dimensional E-Ink Model

Assume the blue dye emulsion has a random distribution of white pigment balls and micelles (Fig. 3). Given an applied field $\mathbf{E} = E_x\ \mathbf{i}$, the two species in the dispersion undergo charge separation as each migrates towards the electrode of the opposite polarity. Simulation parameters m, q, η, and r represent mass, charge, number and radius, respectively, for pigment and micelle denoted with subscripts p and m. The remaining quantities η, E_x and Δt are dye viscosity, electric field, and time-step size. Using parameters defined in Fig. 3, the two species are tracked from rest to compute their velocity as plotted in Fig. 4. For a capsule diameter of d = 120 µm and a terminal velocity of 170 µm/s, the estimated pigment transit time is $\tau_{transit} = 0.7$ sec; which is much longer than the acceleration time of 2 µs. Hence, instead of integrating the force equation over time, a simpler approximation is to use the drift velocity with a mobility defined as the velocity per unit $\mathbf{E}$ field: $\mu_{pigment} = v_\infty/E_x = 1.7 \times 10^{-5}$ cm²/V.s. This is a useful method to calculate particle mobility from first principles.

Analytic Estimates of Terminal Velocity (v_∞) and Acceleration Time (τ)

Newton's equation of motion for the E-Ink pigment may be written as:

$$dv/dt = (qE/m) - (6\pi\eta r/m)\ v\ =\ \alpha - \beta v \qquad (6)$$

The solution of this first order ordinary differential equation is:

$$v(t) = \alpha/\beta\ (1 - e - \beta t) \qquad (7)$$

and expressions for terminal velocity and switching time are:

$$v_\infty = \alpha/\beta = qE/6\pi\eta r \qquad \tau = 1/\beta = m/6\pi\eta r \qquad (8)$$

The analytic solution in Eq. (7) for pigment velocity is also plotted in Fig. 4 to show excellent agreement with the numerical solution. The pigment time constant is in microseconds compared to the corresponding time constant for the micelles, which is in nanoseconds.

Simulation Parameters:

$m_p = 4.3983 \times 10^{-12}$ gm
$q_p = +1.6022 \times 10^{-17}$ C
$n_p = 1$
$r_p = 1$ um
$m_m = 4.0317 \times 10^{-16}$ gm
$q_m = -1.6022 \times 10^{-19}$ C
$n_m = 100$
$r_m = 0.05$ um
$\eta = 5. \times 10^{-4}$ kg.m/s
$\Delta t = 1.0$ us
$E_x = 0.1$ V/um

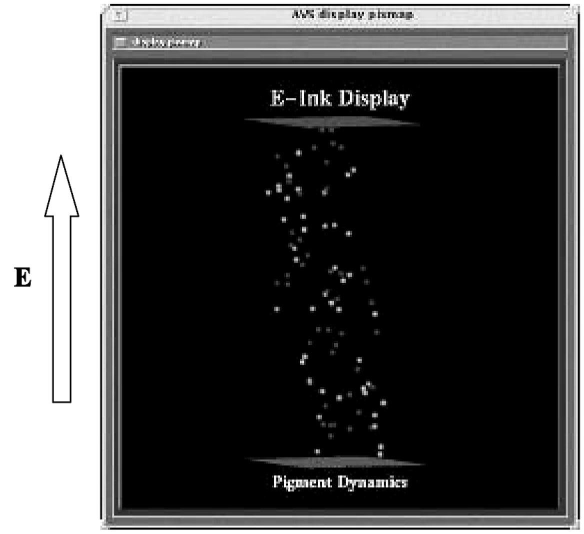

Figure 3. E-Ink simulation parameters and AVS rendering showing larger pigments and smaller micelles moving in opposite directions due to the bias E field

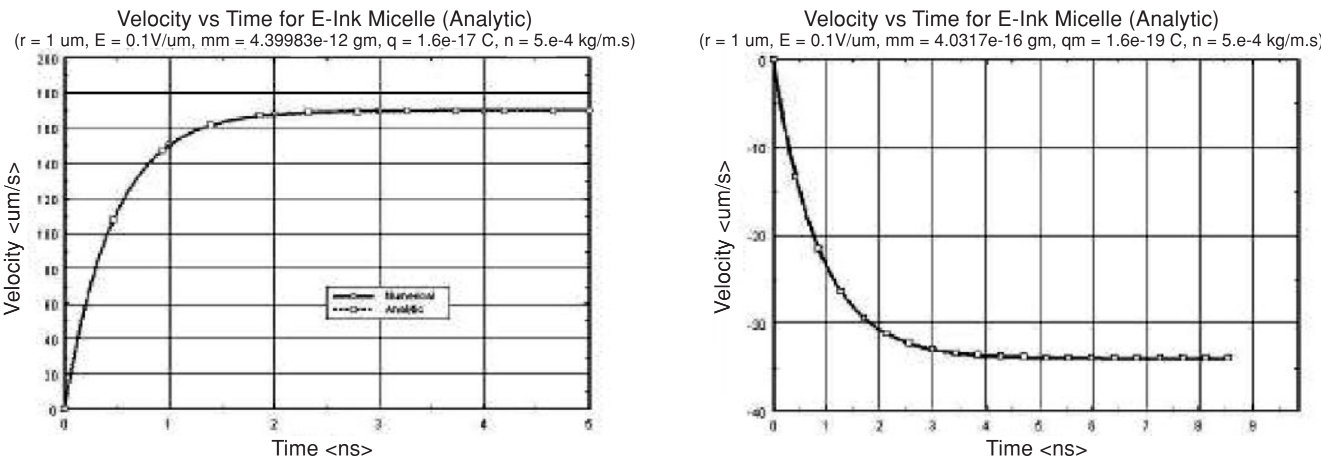

Figure 4. Model predictions of E-Ink pigment (left) and micelle (right) transient velocities

E-Ink Laboratory Experiments

Figure 5 shows the experimental setup for an E-Ink "quad laminate". Each 4″ × 8″ laminate consists of four slanted panels and each panel is divided into 63 addressable electrode regions, which can be individually or collectively switched to produce combinations of the desired display shapes or characters.[13] Adhesive Cu tape was used to make electrical connection to a HP function generator programmed to output a bipolar square wave at 1 Hz and 160 mV peak-to-peak. The output was fed into a Trek 1:1000 voltage amplifier to produce the ±80 V needed to drive the display. A microscope was used to examine the switching of cells.

Figure 6 shows some snapshots of experiments saved with a frame-grabber on a PC. The top row shows the test cell and instrumentation. In the second row, the left picture shows the characteristic "ring of white" on the inside of each capsule due to image fading when the field is switched off for a few seconds. The rings result when the stacked pigment particles remain attached to the vertical capsule walls while those at the top are detached from the viewing surface. This observation shows that the image is volatile. The picture on the right shows "cross-talk" or edge smearing when a capsule straddles two adjacent electrodes. Interference due to the **E** field from the adjacent electrode acts to blur the edge between blue and white regions. The two pictures in the third row show the two extremes of the display, contrasting the blue dye background against the white pigment image. The bottom row shows results of a frequency scan from 1 Hz to 20 Hz to study the relaxation time of the display. At 1 Hz, the display appears to refresh with no apparent history effects. As the frequency is increased the motion of the white pigments become jerkier. Above 7 Hz, the dye appears to be agitated by the motion of the white pigments due to electrohydrodynamics (EHD). The motion of the pigment creates a drag on the dye. The subsequent flow of the dye redistributes the pigment thus coupling dye flow and pigment motion. As the frequency is increased, the rapid switching prevents the pigments from sticking to the walls as their directions are reversed before they complete migration, leading to a stirring or sloshing motion. The two figures are snapshots taken at 10 Hz and 20 Hz, respectively.

Figure 7 shows representative static and dynamic reflectivity measurements of the electronic media using a

TABLE I. Normalized Static Reflectivity Measurements for E-Ink and Gyricon Samples

E-Ink			Gyricon red/white			Gyricon black/white		
%White	%Blue	Contrast	%White	%Red	Contrast	%White	%Black	Contrast
0.39	0.07	5.57	0.28	0.12	2.33	0.31	0.09	3.44

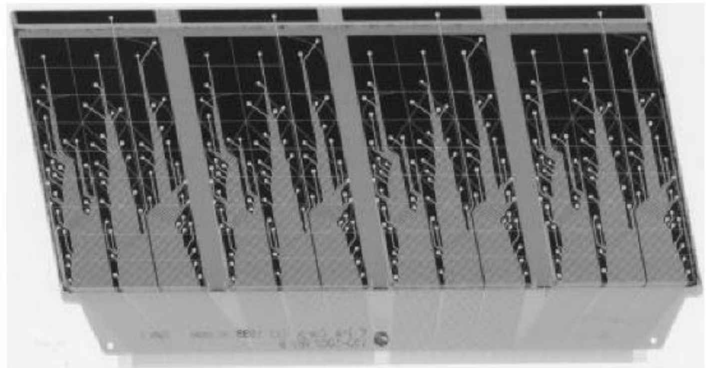

Figure 5. E-Ink experimental setup and rear electrode connections for "quad laminate".

Gretag SpectroScan with a PC interface. The sensor is initially calibrated against a reference white spot prior to taking the optical density CMYK readings shown in Table I. Contrast is the ratio of white to background dark reflectance with a large number indicating better visibility. Dynamic optical measurements are useful to indicate transient switching information. Since the time constant is less than 1 sec, the speed of the photodiode has to be much faster. Figure 7 also shows a set of data, taken at 4 ms intervals with an AC bias of ±90 V. The three 600 ms half-cycles show that reflectance lags behind the relatively instantaneous electrical waveform. The time constant of 0.6 s agrees well with the model prediction of 0.7 s for pigment transit time. The lead edge (white) of the waveform is not symmetric with the trail edge (blue) due to the difference in pigment motion. For white, the pigments jostle each other as they approach the upper electrode, causing some delay in settling of the measured reflectivity. For blue, the pigments are all repelled at once from the upper electrode, causing the reflectivity to drop off more sharply.

Sample Calculation with 3-Dimensional Gyricon Model

Assume the Gyricon dipole is initially oriented at $(\theta,\psi) = (30,-90)$. When a field $\mathbf{E} = E_x\,\mathbf{i}$, is applied, the dipole rotates in a few milliseconds to the final orientation of $(\theta,\psi) = (90,0)$. Simulation parameters m, q, and r refer to the mass, hemispherical charge, and radius of the bichromal ball. The remaining parameters: η, E_x and Δt are as defined previously. Using the specified parameters (Fig. 8), damping constant k is estimated from the following analytic solution, and used to calculate the transient switching curve shown in Fig. 9.

Analytic Estimates of Damping Constant (k) and Switching Time (τ)

The two equations that specify the Gyricon ball orientation are:

$$mr^2\, d^2\theta/dt^2 = pE_x \cos\theta - k4\pi\eta r^3\, d\theta/dt$$
$$mr^2\, d^2\psi/dt^2 = -\,pE_x \sin\theta \sin\psi - k4\pi\eta r^3\, d\psi/dt \quad (9)$$

Particular solutions corresponding to the preceding model calculation are:

$$\psi(t) = -90\, e^{-t/\tau} \qquad \theta(t) = 90 - 60\, e^{-t/\tau} \quad (10)$$

The time constant and damping coefficient are derived as:

$$\tau = \sqrt{(mr/8qE_x)} \quad k = 1/\pi r\eta\sqrt{(qE_x m/2r)} \quad (11)$$

Figure 9 plots the analytic solution together with the results from the numerical model. The only difference in the curves is the effective time constant, which is underpredicted by the model due to truncation error as only the first term in the series expansion for sin ψ is used.

Comparison with Published Gyricon Results

Sheridon[8] measured Gyricon ball switching time versus ball diameter for three **E** field levels. The Gyricon model is used to compute results for comparison. The charge distribution is assumed to vary as $q/q_o = (r/r_o)^n$, so that $q/m = q_o/m_o\,(r/r_o)^{n-3}$.

When $n = 3$, q is distributed uniformly through the volume of the ball. Then,

$$q/m = q_o/m_o = \text{constant} \qquad \tau = \sqrt{(m_o r/8q_o E_x)} \Rightarrow \tau \propto \sqrt{r} \quad (12)$$

When $n = 2$, q is distributed on the surface of the ball. Then,

$$q/m = q_o/m_o\,(r/r_o)^{-1} \quad \tau = \sqrt{[(m_o r/8q_o E_x)(r/r_o)]} \Rightarrow \tau \propto r \quad (13)$$

When $n = 1$, q is only partially distributed on the surface of the ball. Then,

$$q/m = q_o/m_o\,(r/r_o)^{-2} \quad \tau = \sqrt{[(m_o r/8q_o E_x)(r/r_o)^2]} \Rightarrow \tau \propto r^{3/2} \quad (14)$$

Comparing with Sheridon's data plotted in Fig. 10, it is clear that the exponent n lies in the range: $1 < n < 2$, and may be extracted as shown in Table II from:

$$n = 3 + \ln\,[(r/8E_x\tau^2)/(q_o/m_o)]\,/\,\ln\,(r/r_o) \quad (15)$$

The abstracted values clearly agree very well with theoretical prediction. Average values of n = 1.1, 1.4, and 1.8 corresponding to **E** field levels of 3.4, 6.9, and 10.3×10^3 V/cm, respectively, were used by the Gyricon model to generate curves shown in Fig. 10 for compari-

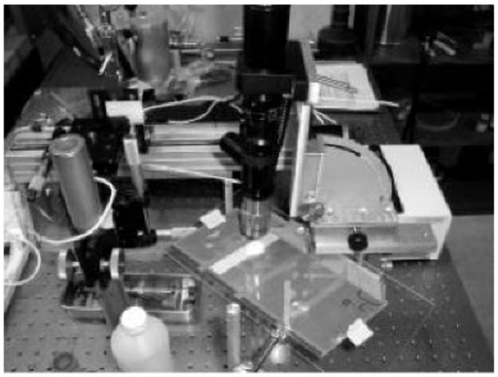

Test cell setup

Bench top electronics setup

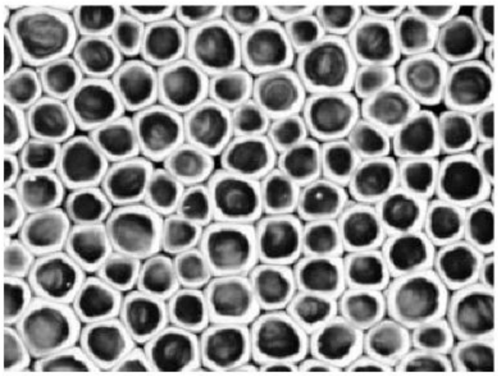

Image fading after 10 seconds with **E**=0

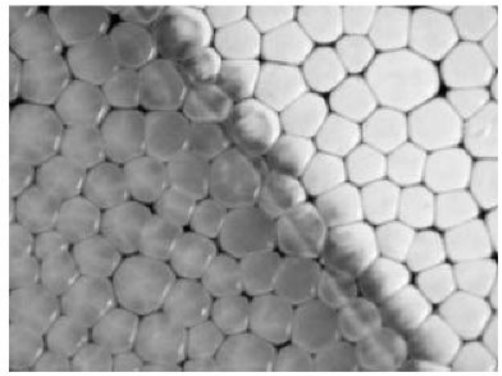

Image edge smearing or cross-talk

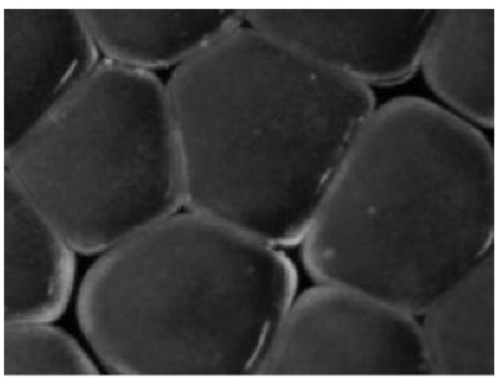

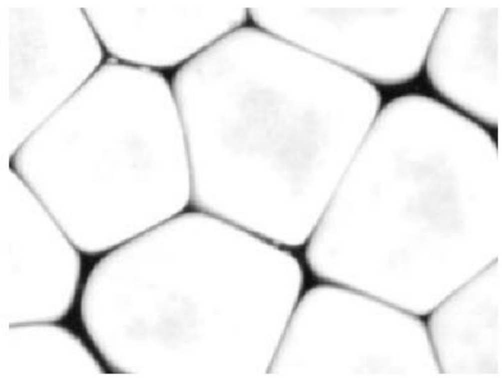

Blue dye background (left) and white pigment image (right) regions showing high image contrast

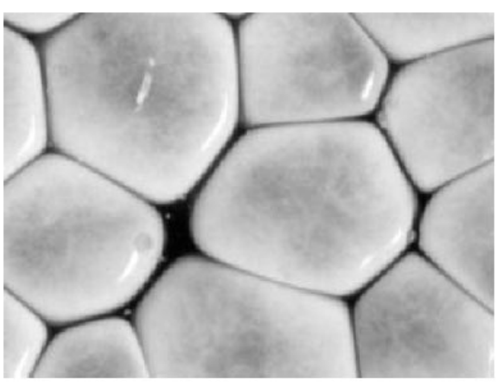

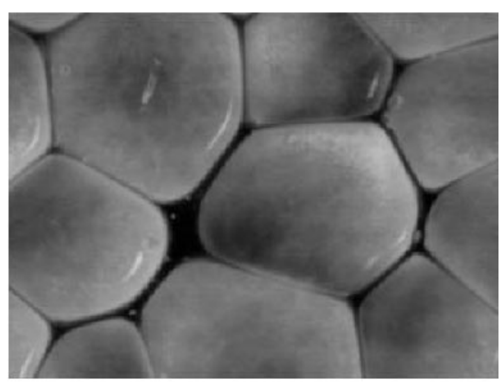

Switching at 10 Hz (left) and 20 Hz (right) showing gray levels due to EHD flows.

Figure 6. Experimental setup and micrographs for E-Ink sample

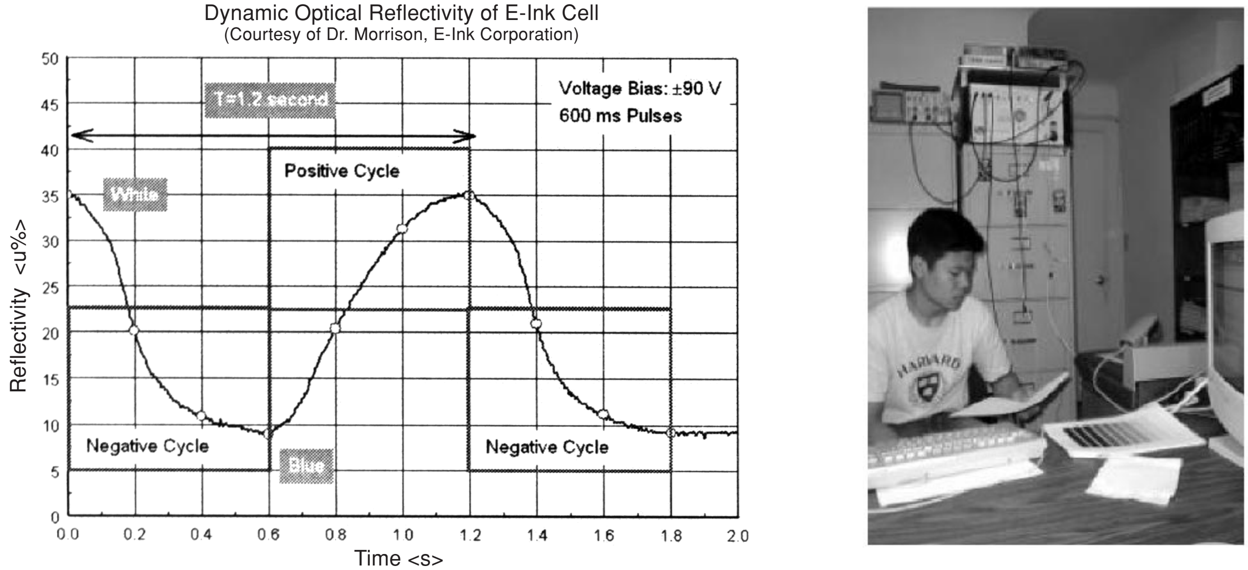

Figure 7. Dynamic and static reflectance measurements of E-Ink display cells.

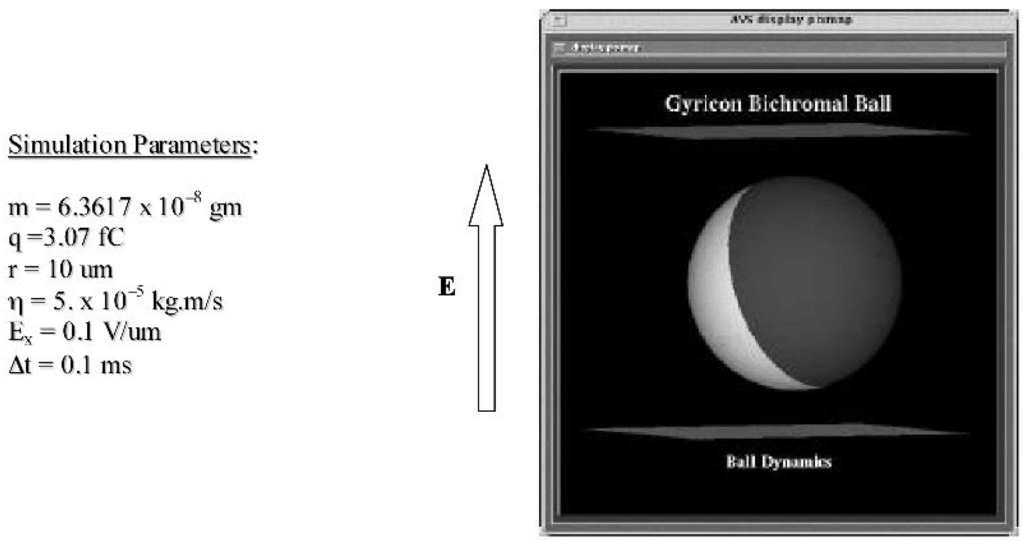

Figure 8. Gyricon simulation parameters and AVS rendering showing red/white bichromal ball rotating due to the torque induced by the bias E field

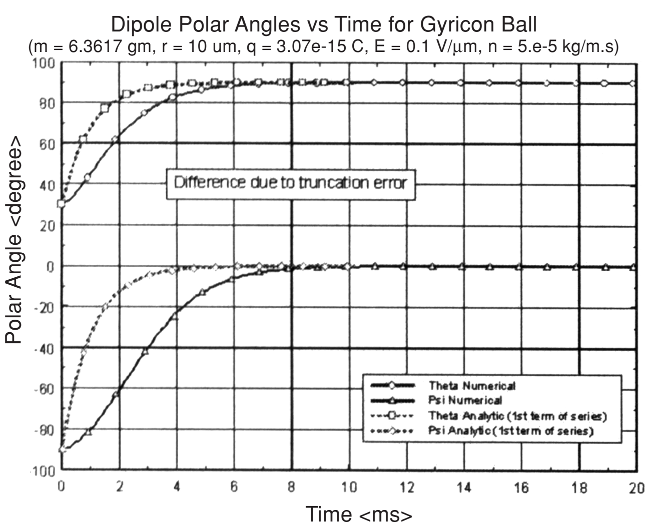

Figure 9. Model prediction and analytic results for transient response of polar angles θ and ψ

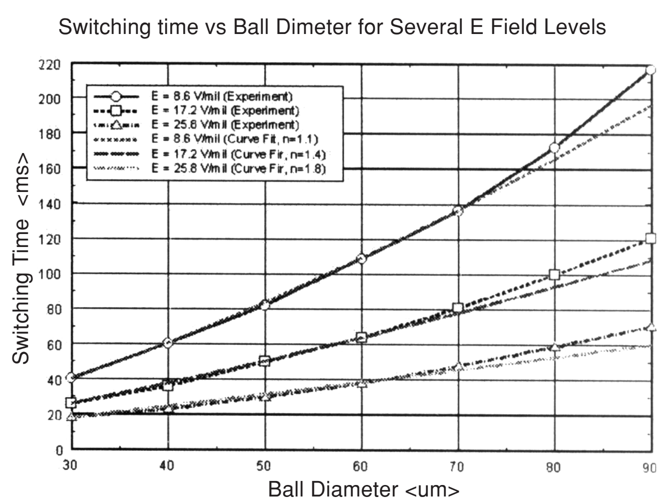

Figure 10. Comparison of model prediction and Sheridon's switching time versus ball size data

Bench top experimental setup

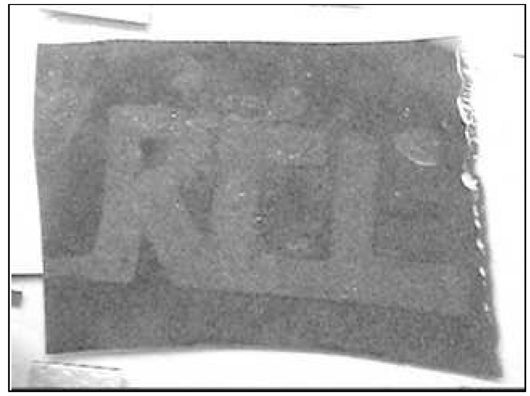

Gyricon as a display – "RCL"

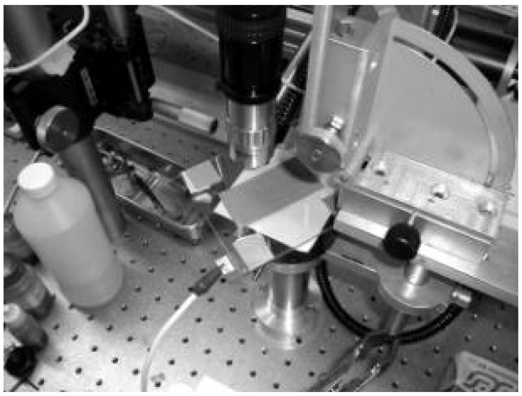

Display cell of red/white sample

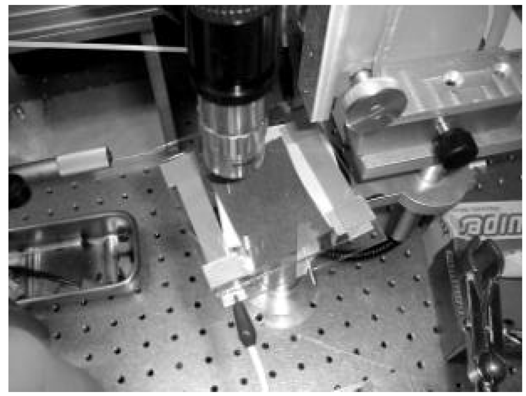

Display cell of black/white sample

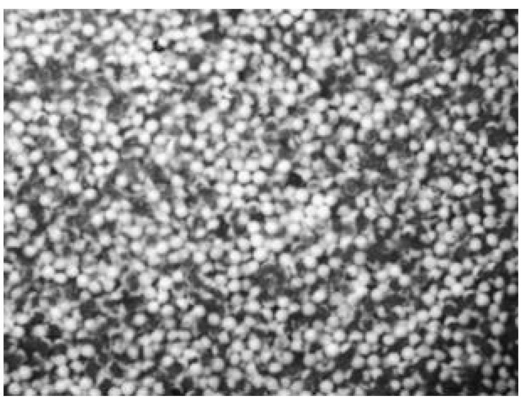

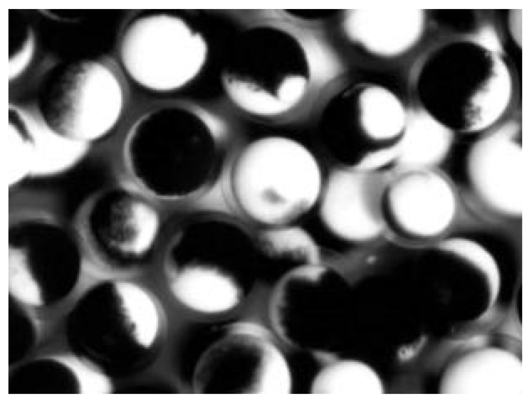

Magnified red/white (left) and more magnified back/white (right) Gyricon samples

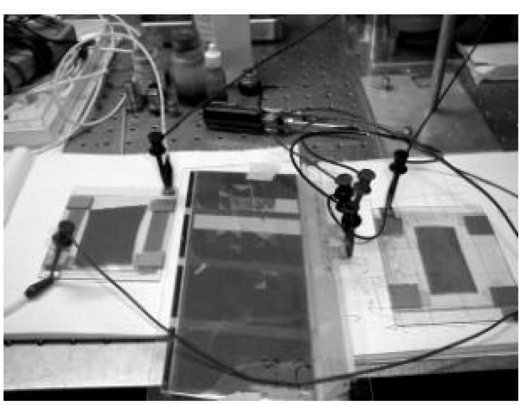

Three display cells in series.

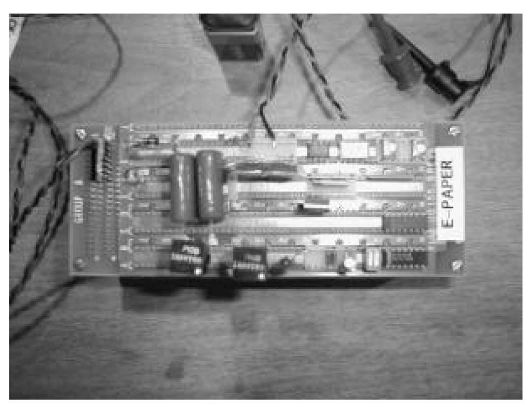

Portable 9V display driver circuit.

Figure 11. Experimental setup and micrographs for Gyricon samples.

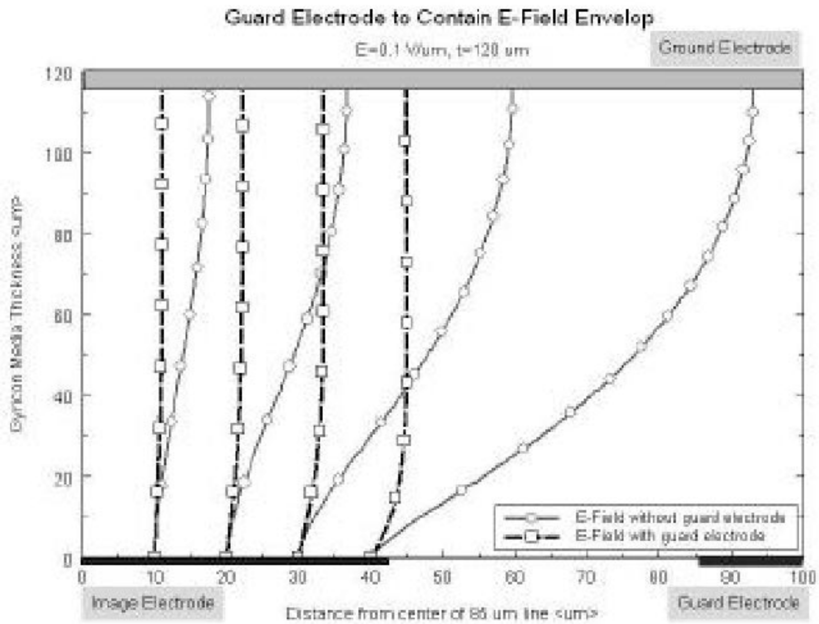

Figure 12. Line broadening due to fringing edge E fields are obtained from solution of Laplace's equation, shown by the four spread out tracers. The four bunched tracers show very little spreading when an adjacent electrode is placed one half line width away (on the right) to compress the E field lines.

TABLE II. Exponents *n* Extracted from Sheridon's[8] Experimental Gyricon Switching Data

d<µm>	n E = 3.4 x 10³ V/cm	n E = 6.9 x 10³ V/cm	n E = 10.3 x 10³ V/cm
40	1.1811	1.7376	2.2959
50	1.1895	1.4397	2.0000
60	1.1075	1.4009	1.8440
70	1.1113	1.3177	1.6848
80	1.0258	1.2532	1.5793
90	0.9215	1.2007	1.5017

son with the original experimental plots. Agreement is excellent for ball diameters up to 70 µm.

Gyricon Laboratory Experiments

The two Gyricon samples tested are red/white and black/white.[14] The experimental setup shown in Fig. 11 is identical to the E-Ink case. The two samples are shown in the second row. The test material is a 0.015 in. thick elastomer, which is soaked in Isopar for several hours to have the fluid absorbed into the cavities. Display cells are fabricated by laying the material between two pieces of NESA glass with the conductive sides facing in. Two 0.005 in. Teflon shims are used as spacers to prevent the two NESA glass pieces from contacting. Adhesive Cu tape is used to form contact pads on the glass. The entire test cell assembly is then held together with duct tape. Magnified images are shown in the third row. The samples are tested to observe ball rotation or switching due to the applied torque. Both samples needed ±80 V from rest to overcome stiction but once started, the voltage may be reduced to ±50 V to sustain ball rotation. Frequency scan from 1 Hz to 20 Hz shows results similar to the E-Ink sample. A stopwatch together with the scan frequency was used to estimate switching times.

The top row right picture shows an experiment where the biased electrode is shaped to display a flashing "RCL" logo cut out from 0.001 in. thick Aluminized Mylar. The physical size of the logo is smaller than the displayed image. The reason for this magnification is that the applied **E** field at the electrode edge broadened outwards in going through the Gyricon material leading to "image blooming", i.e., bichromal balls, within this field either fully or partially rotate.

Figure 12 shows the distribution of field lines from a two-dimensional **E** field analysis, computed by tracking four arbitrary tracers with velocity given by the local **E** field. An 85 µm wide line can broaden to 190 µm through a 120 µm thick Gyricon media as shown by the outer line. With a guard electrode placed 42.5 µm away, the **E** field lines are compressed so that there is no noticeable line broadening as shown by the essentially vertical tracers. In Fig. 11, the bottom row right picture shows a portable circuit constructed to replace the entire bench top of equipment. The circuit is fabricated from two Pico DC/DC step-up converters that take the voltage input from the 9V battery and outputs the ±150 V range. A programmable IC (PIC) is coded with the required test frequency range: 0.2, 1, 2, 4, 8, 10, 15, and 20 Hz. The circuit design minimizes capacitive loading, allowing a 9V battery to run continuously for many hours.

As additional verification, the Gyricon model is exercised for various values of k, and results are summarized in Table III and Fig. 13. Over-damped systems lead to prolonged settling time, τ_∞, and therefore adversely affects refresh rate. Under-damped systems converge slowly to multiples of 360 degrees due to over rotation. The optimum k is chosen to critically damp the system.

Suggestions for Performance Optimization

Several notions are proposed to improve on the performance of the two displays.

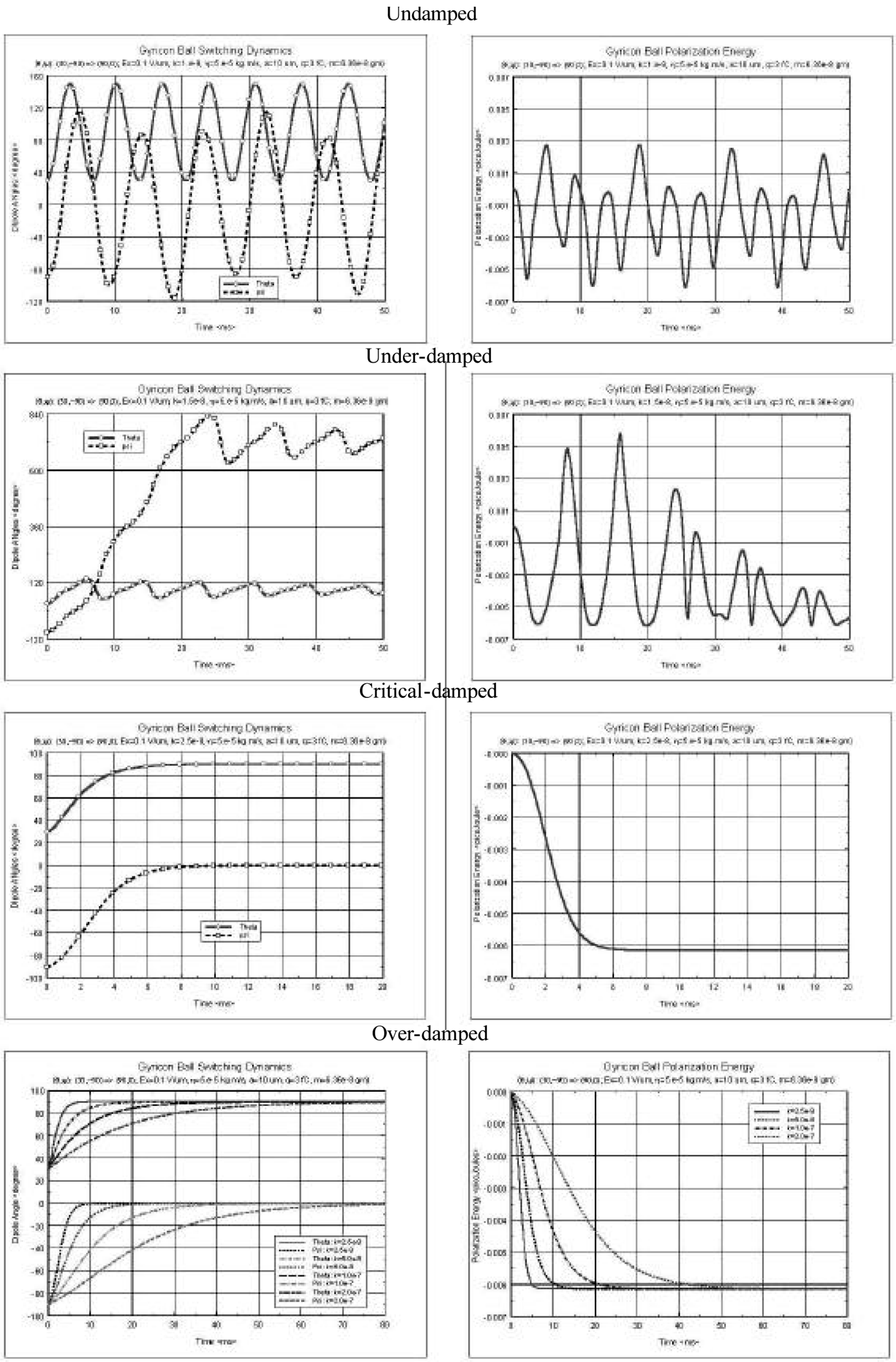

Figure 13. Gyricon model predictions for transient response of polar angles (left) and polarization energy (right) for range of viscous damping constants

TABLE III. Gyricon Model Behavior with Test Range of Damping Constants

Cases	k	τ_∞	Remarks
Undamped	0.7958	—	Both (θ,ψ) oscillating; ψ modulated
Under-Damped	7.9580	—	Converging oscillations, $\psi \rightarrow 1440$
	11.9370	—	Converging oscillations, $\psi \rightarrow 720$
	15.9140	—	Converging oscillations, $\psi \rightarrow 0$
Transition	17.9055	6.5 ms	Minor oscillation after convergence
Critical-Damped	19.8950	7.5 ms	Converge without oscillations
Over-Damped	39.7900	15.0 ms	
	79.5800	30.0 ms	
	159.1600	60.0 ms	

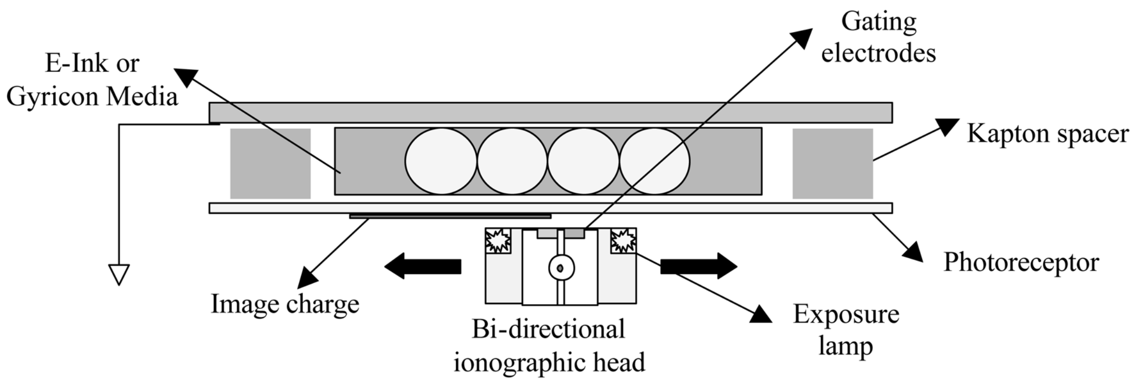

Figure 14. Setup for ionographic image charge printing to create higher resolution display

Lower Switching Voltage

The **E** fields through the thin display samples are very linear or one-dimensional for both the E-Ink and Gyricon samples. Reducing the thickness of the sample by a factor of 5 will proportionally lower the driving voltage to less than 18 V, while maintaining the **E** field level. This scheme allows the use of less expensive driver chips and extends the time of operation for portable batteries or voltage sources.

Faster Display Switching

Faster switching leads to more rapid refresh rates. Both display media operate on principles that require separate considerations. The analytic solutions derived provide mathematical relationships that can be used to optimize design. For E-Ink, faster switching in Eq. (8) implies that the terminal velocity should be increased by increasing pigment charge and switching field and/or decreasing pigment size and dye viscosity. For Gyricon, faster switching in Eq. (11) translates into a faster (smaller) switching time constant for the critically damped case, or a reduction in ball mass and size while increasing ball charge and switching field. The critical damping constant, k, provides an explicit relationship between viscosity, **E** field, and ball charge, mass and size; inferring that switching time is inversely proportional to viscosity of the plasticizing fluid.

Increase Display Resolution

At a monochrome resolution of 80 dpi, 6400 electrode connections are needed per square inch for active matrix addressing of every pixel. For color, this number is increased to nine times, resulting in a prohibitive number of connections. A scheme is proposed to substitute ion charge for electrode voltage to sustain the local E field needed to switch the display. Imagine that charge is printed on a dielectric sheet in much the same way that an ink jet printer is used to create a hardcopy output on paper. The result is a continuous toned latent image that is restricted in resolution only by the size of the pigment capsule and the resolution of the ion print head. The amount of charge necessary to produce a field equivalent to 1.0 V/μm may be estimated by a capacitance calculation, assuming $\varepsilon_r = 3$, to be 2.65 nC/cm^2, which represents a very small amount of charge for a corona device. The conceptual implementation of this idea for both E-Ink and Gyricon is shown in Fig. 14. An ionographic print head is used to deliver ions to the lower surface of the two-layer structure composed of a dielectric layer and the electronic display media. The upper NESA glass provides the ground reference. The pair of electrodes at the exit of the ionographic head modulates the ions by applying a cross field to turn the ion flow on and off, resulting in a latent image charge being continuously deposited or printed onto the photoreceptor. The photoreceptor is an ideal dielectric or insulator in the dark, but when flash exposed becomes a good conductor and the charge is leaked off to erase the image. For bi-directional use, flash lamps are attached on both sides of the scanning print head to erase the previous image.

Controlled Induction Charging of Gyricon Balls

The chemical mechanism used in the charging of bichromal balls is a trade secret. The charge imbalance in the two hemispheres greatly affects ball dynamics, so controlling this imbalance is an important design criterion. A method is proposed for inductive charging that would produce controlled amounts of equal and opposite charge on the two hemispheres of

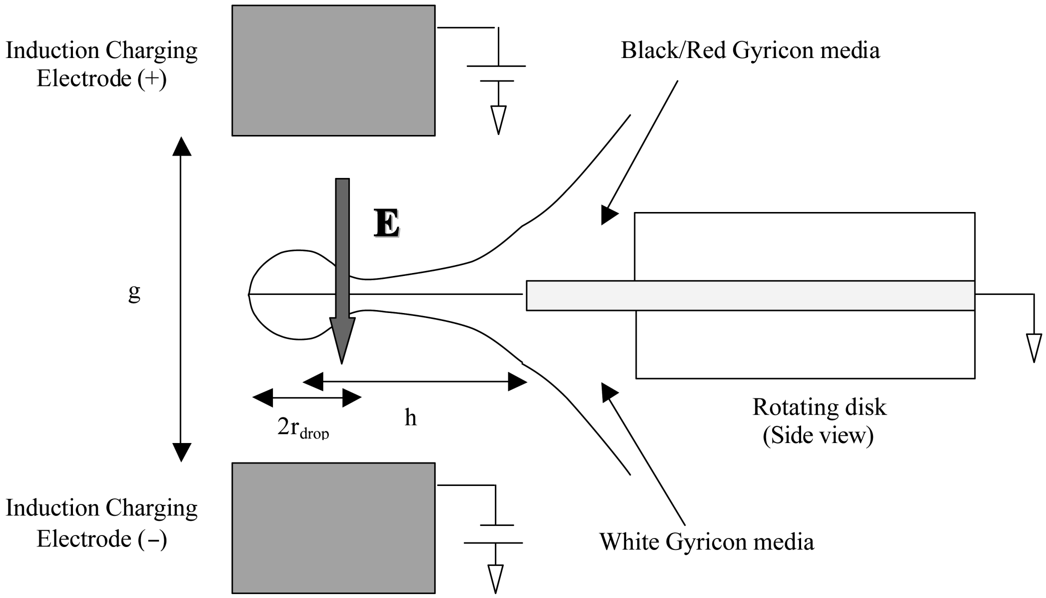

Figure 15. Setup for controlled induction charging of Gyricon bichromal ball

TABLE IV. Sample Electrical Properties for Controlled Charging of Gyricon Material

r_{drop} (μm)	E (V/μm)	$\lvert Q_+ \rvert = \lvert Q_- \rvert$ (fC)	σ_{media} (mho/cm)	ρ_{media} (Ω–m)
10	1.0	5.5631	2.833×10^{-7}	10^4

the ball. The configuration is shown in Fig. 15, and builds on a previous publication by Richley[10] where balls are fabricated using the fluid dynamic instability of the waxy material on a spinning disk or rotary atomizer. The idea is to inductively charge the drop at the point of break-off. A pair of electrodes spaced a gap, g, apart is used to set up a linear transverse E field as shown. The grounded Gyricon material has a minimum electrical conductivity such that the charge relaxation time constant is much less than the hydrodynamic time constant for ball formation. Within the gap, a small voltage is induced on the ball surface which leads to an approximate equation for charge on each hemisphere: $Q\pm = \pm 2\,\pi\,\varepsilon_o\,r_{drop}{}^2 E$. Ball fabrication rate determines an RC charging time (τ_{drop}), which is then used to specify the conductive and resistive properties of the material. For $r_{drop} = 10$ µm, $\tau = 10$ µs, and $E = 1$ V/µm, the designed media properties are shown in Table IV.

Image Gray Level Control

In Gyricon, gray level control can be achieved by partial ball rotation. This may be realized by introducing a non-zero net charge, which leads to a Coulomb force that also translates the ball. When the ball contacts the cavity surface, it will stop rotating due to wall friction. By designing the cavity size in relation to the ball size, the ball can be under rotated to achieve gray levels. In the case of E-Ink, an analogous scheme for gray level control is to vary the bias voltage, which also linearly varies the amount of pigment deposited onto the viewing surface thus creating the perception of image gray levels.

Conclusions and Future Work

This article has described the physics and development of numerical models to simulate the dynamic performance of both E-Ink and Gyricon electronic paper technologies. Models have been verified against analytic solutions, published data, and laboratory experiments. Experiments also pointed out imaging artifacts such as line broadening which may be minimized through electrode design. Excellent agreement was shown with a set of self-consistent device parameters. Animation of the solution dynamics using AVS compared very well with experimental video. Verified models were used as engineering design tools to explore trade-offs and optimize display performance. Specific ideas were proposed to: lower switching voltage, reduce switching time, improve display resolution, control Gyricon charging, and create gray level images.

Some qualitative comparisons may be drawn between the two versions of electronic paper. E-Ink display has higher contrast and therefore image visibility but the 120 µm microcapsule restricts the image resolution to about 220 dpi. Gyricon has better resolution but lower contrast; a result that is not intuitive from multiple layers of reflecting balls. In experiments, only the top two layers showed active switching. One reason may be that Isopar is inferior to the low viscosity silicone oil that Sheridon uses.[14] Another could be the lower contact pressure on the elastomer, as Teflon shims were used to maintain a minimum separation between the two plates. This could lead to air gaps, which would weaken the switching **E** field. Gyricon images are experimentally observed to be non-volatile, and do not change unless power is reapplied. For a short duration of between 5 to 10 sec, E-Ink images are also somewhat non-volatile. The primary concern is the displacement current, a term proportional to $\partial E/\partial t$, due to the time-varying **E** field as in rapid switching. This current represents a capacitive load, which may act to limit switching speed. Both versions of electronic paper have shown good promise and attracted much media attention.[15] The next few years will be crucial as they evolve to fill the recognized need in many diverse markets. Much interest have also been shown recently by many researchers as evidenced from the literature.[16–23]

A natural extension of this work is to apply the models to answer specific questions on display performance.

Another is to guide the implementation of some or all of the proposed improvements. Yet another extension is to simulate color display devices using a triplet of physical pixels together with three RGB filters per image pixel; a scheme which would effectively reduce resolution by 3 times.

Acknowledgment. The author is indebted to the following for their support, guidance, and counsel in the course of pursuing this research: Dr. Nicholas Sheridon, Chief Technologist, Gyricon Media, Inc.; Dr. Ian Morrison, Director of Ink Research, E-Ink Corporation; Mr. Joseph Sencen, Adviser, Intel Science Research Project; Mrs. Joyce Kelly, Physics Teacher; Dr. Meng H. Lean, Xerox Corporation; and Mr. John Ricciardelli, Xerox Corporation. In particular, Dr. Nick Sheridon and Dr. Ian Morrison are thanked for providing valuable samples, hosting visits to Palo Alto, CA, and Cambridge, MA stimulating and enlightening discussions and consultations, and reviewing the draft manuscript.

References

1. J.P. Wheeler, Light emitting polymers are ready for prime time, *Photonics Spectra* **31,** 130 (1997).
2. T. Hatano, N. Kobayashi, M. Okada, and K. Hashimoto, Bistable paper-white display device using cholesteric liquid crystals, *Proc. SID*, 269 (1996).
3. P. Kolodner, Electronic ink from modified bacteriorhodopsin, *Bull. Amer. Phys. Soc.* **42,** 448 (1997).
4. P. Kolodner, E. P. Lukashev, Y-C. Ching, and D. L. Rousseau, Electric-field-induced Schiff-base deprotonation in D85N mutant bacteriorhodopsin, *Proc. Nat. Acad. Sci.* **93,** 11618 (1996).
5. C. Wu, Bacteria give new meaning to computer bug, *Science News* **151,** 140 (1997).
6. J. Jacobson, B. Comiskey, C. Turner, J. Albert, and P. Tsao, The last book, *IBM Systems J.* **36**(3) (1997).
7. E-Ink web site, http://www.eink.com/
8. N. K. Sheridon and M. A. Berkovitz, The Gyricon—a twisting ball display, *Proc. SID*, Boston, MA, 289 (1977).
9. Gyricon Media web site, http://www.gyriconmedia.com/
10. E.A. Richley, Manufacturing techniques for bichromal balls, private communication, January 2000.
11. Advanced Visual Systems, Inc., *AVS 5.0 User's Manual*, Waltham, Massachusetts, 1996.
12. R. Hayt, *Engineering Electromagnetics*, McGraw-Hill, New York, 1974.
13. I. Morrison, private communication, January 2001.
14. N. K. Sheridon, private communication, July 2000.
15. S. Ditlea, The electronic paper chase, *Scientific American*, 50 (November 2001).
16. R. Sprague, The present and future of Gyricon electronic paper displays, *Proc. NIP17: Int. Conf. on Digital Printing Technologies*, IS&T, Springfield, VA, 2001, pp. 519–522.
17. I. Morrison, E-Ink display, *Proc. NIP17: Int. Conf. on Digital Printing Technologies*, IS&T, Springfield, VA, 2001, pp. 523–525.
18. T. Kitamura, Gug-Rae Jo, and K. Hoshino, Response time for toner display by electrical particle movement, *Proc. NIP16: Int. Conf. on Digital Printing Technologies*, IS&T, Springfield, VA, 2000, pp. 110–112.
19. M. Yasuda, Gug-Rae Jo, K. Hoshino, and T. Kitamura, Role of charge transport layer in toner display by electrical particle movement, *Proc. NIP17: Int. Conf. on Digital Printing Technologies*, IS&T, Springfield, VA, 2001, pp. 744–747.
20. H. Arisawa, H. Harada, T. Kakinuma, T. Hikichi, N. Hiji, M. Koshimizu, T. Ishii, S. Yamamoto, H. Kobayashi, and D. Tsuda, Photoaddressable electronic paper using cholesteric liquid crystal, *Proc. NIP17: Int. Conf. on Digital Printing Technologies*, IS&T, Springfield, VA, 2001, pp. 526–529.
21. T. Takahashi, Y. Kohrin, T. Hayakawa, Y. Toko, and Y. Iwakura, Evaluation of particle velocity in mobile fine particle display with liquid crystal, *Proc. NIP17: Int. Conf. on Digital Printing Technologies*, IS&T, Springfield, VA, 2001, pp. 752–755.
22. Y. Toko, Y. Iwakura, Y. Kohrin, T. Hayakawa, and T. Takahashi, A new type of display for electric paper using fine particles dispersed in the nematic liquid crystal cell, *Proc. NIP17: Int. Conf. on Digital Printing Technologies*, IS&T, Springfield, VA, 2001, pp.748–751.
23. K. Ogura, M. Omodani, Y. Takahashi, and H. Kawai, Microcapsule electrophoretic display method using ion projection head, *Proc. NIP15: Int. Conf. on Digital Printing Technologies*, IS&T, Springfield, VA, 1999, pp. 266–268.